

Online Estimation Variables for the Analysis of Ground Vehicle Inertia Properties

G Veerendra Kumar, Abdul Azeez, B Venkatesh

Swarnandhra College of Engineering & Technology

Department of Mechanical Engineering

Abstract

Vehicle characteristics have a substantial impact on handling, stability, and the propensity to topple over. Two methods for estimating the inertia values of a ground vehicle in real time are presented in this study. In order to account for the uncertainties, the uncertain vehicle model uses the Generalized Polynomial Chaos (gPC) approach, which yields a probability density function for every variable. If one wants to estimate the values of the parameters, they may employ any number of statistical methods to these PDFs. This case employs the Maximum A-Posteriori (MAP) estimator. The MAP estimate maximizes the distribution of $P(z)$, but where is the vector of parameter PDFs and what is the observable sensor comparison? Applying an adaptive filtering method is an additional option. The Kalman Filter is one kind of adaptive filter. It is possible to update the parameter distributions' PDFs at each time step by integrating it with the gPC theory. The median values of these PDFs are adjusted by the filter to be closer to the actual values.

Introduction

The robust design of vehicle control systems allows them to withstand inaccurate parameter values. When you load and unload the car, it generates these erroneous parameter values. Normally, this wouldn't be a major concern, but in the case of stopping vehicles from flipping over, it might have catastrophic consequences. More accurate parameter measurements are beneficial to control systems because to the discontinuity nature of vehicle rollovers.

Estimating these changes and providing updates for the on-board systems are the goals of this study. It is important to consider many factors. First things first: figure out how you'll get your data. The second is picking a model

that can forecast the important parameters with less data. Our research presents two methods that may be used independently of a terrain profile to calculate the mass and moment of inertia of a vehicle while it is in motion in two dimensions (pitch and roll). To accomplish our objectives, we use Bayesian statistics in conjunction with a combination of the Extended Kalman Filter and the mathematical strategy of Generalized Polynomial Chaos.

as gPC. The computational efficiency of estimating parameter uncertainty is enhanced by the Generalized Polynomial Chaos method [4, 12, 23, 24].

A Review of the Existing Literature The methods used to estimate parameter values are as diverse as the fields in which they fall. Possibly, features of electrical gadgets are the important considerations [11]. There are a plethora of effective methods for making estimates, such as Genetic Algorithms, Lyapunov Stability, Kalman Filtering, and many more [1, 13, 14, 17, 21]. Parameter estimate in vehicle dynamics is similar to parameter estimation in other domains [6]. Possible unknowns include vehicle mass, inertia, aerodynamic drag coefficient, spring stiffness, suspension damping, and a host of others. An approximation of the vehicle's mass and moment of inertia is computed using a variety of methods. To determine the mass of a vehicle, one may take into account factors like the torque produced by the engine, the inertia of the drivetrain, the resistance to wind, the rolling resistance of the tires, and the gradient of the road [7, 13, 21]. As stated in [21], this problem occurs because the evaluation of the vehicle's rolling resistance—a measure that changes non-trivially over time—is especially affected by the estimate of the other parameters. Some methods for estimating various vehicle attributes are shown in [17]. The writers of this

study ascertain the vehicle's mass, horizontal center of gravity, and pitch and roll moments of inertia. Regrettably, this estimate approach relies on the assumption that the road noise is Gaussian white noise, which is not always true. A terrain profile is essential because non-trivial estimate mistakes might result from incorrect anticipated parameters.

Mechanics of Moving Vehicles

Vehicle dynamics often use seven-DOF base excitation models like the one shown in Figure 1. The chassis, also called the sprung mass, is what holds the model's suspension components and wheels together (denoted as unsprung masses). The model first utilizes the tire dynamics to get the unsprung masses excited by the terrain profile, and then it uses the suspension components to get the sprung masses excited. The current research eliminates the need for a specific terrain profile, and the model adds the roll degree of freedom in addition to the vertical bounce and pitch degrees of freedom previously studied in [15]. This is crucial because it would be impossible to determine the roll inertia of the vehicle without taking its roll motion into account.

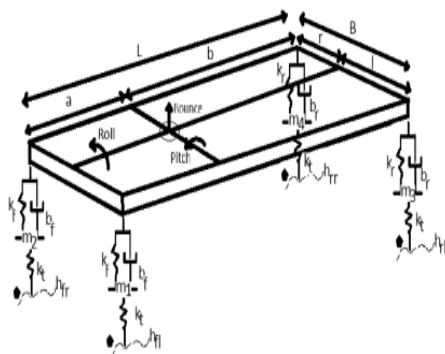
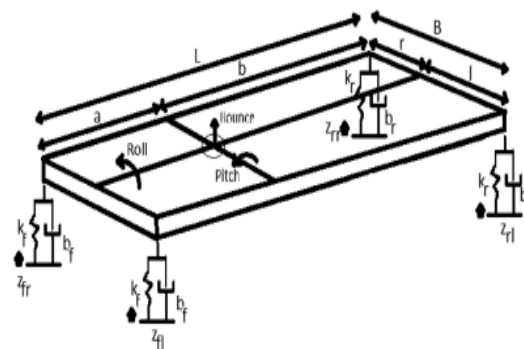


Fig. 1. The seven-DOF vehicle model's dynamics.

The values for the four unsprung masses are denoted by the parameters m_1 , m_2 , m_3 , and m_4 . For tires, that number is k_t , which stands for stiffness. The geometric properties of the sprung mass are described by the parameters a , b , r , l , L , B (where a and b are the distances from the front and rear axles to the center of gravity of the sprung mass, r and l are the corresponding distances from the right and left

sides of the vehicle, and L and B are the wheelbase and track, respectively).

transport system). Front and rear wheel damping and stiffness are represented by the parameters k_f and b_f , respectively. The four vertical acceleration movements of the wheels are used as inputs in the updated model of the seven DOF system. This eliminates the requirement to know the stiffness, weight, and damping of the unsprung masses, as well as the terrain profile, reducing the computational complexity. As seen in Figure 2, this new model allows for the sprung mass to vertically bounce, rotate in the pitch axis, and roll in the yaw axis, for a total of three degrees of freedom.



As shown in Fig. 2, the model's dynamics include three distinct degrees of freedom.

The following assumptions were used in the development of this model: low lateral velocity, low yaw velocity, low longitudinal acceleration, low lateral acceleration, low roll angle, low pitch angle, linear suspension elements, front-and-rear-element symmetry ($k_{fr} = k_f$, $l = k_f$), and low angular accelerations and angular rates.

One "center" is used for the sprung mass, while another is used for the collection of unsprung masses. Height, pitch, and roll of the center of mass determine the "center" of the sprung mass. The geometric mean height, z_u , cg , roll, u , cg , and pitch, u , cg , for each body is used to define the center of gravity for the unsprung masses in this adaptation of the quarter car model; the centers of gravity for the ensemble of the unsprung masses in vertical bounce, pitch, and roll are thus described as:

$$z_{u,cg} = (L-a) \frac{B-l}{LB} z_{fl} + (L-a) \frac{l}{LB} z_{fr} + a \frac{B-l}{LB} z_{rl} + a \frac{l}{LB} z_{rr} \quad (1)$$

$$\theta_{u,cg} = \frac{-(r z_{fl} + l z_{fr}) + (r z_{rl} + l z_{rr})}{LB} \quad (2)$$

$$\phi_{u,cg} = \frac{[(b z_{fl} + a z_{rl}) - (a z_{rr} + b z_{fr})]}{LB} \quad (3)$$

Accelerations are measured by accelerometers on the instrumented vehicle, therefore similar relations to Equations (1), (2), and (3) may be stated in terms of accelerations. The resulting accelerations are used as inputs in the following three equations: (4), (5), and (6). Wheel vertical displacements are denoted by the parameters z_{fl} , z_{fr} , z_{rl} , and z_{rr} , respectively. The sprung mass's dynamic equations of motion are specified by the following, where M_u , J_{pitch} , and J_{roll} are the unknown quantities that represent the sprung mass's mass, pitch inertia, and roll inertia, respectively.

$$M_u \ddot{Z} = \left(\sum_{i=fl,fr,rl,rr} F_i \right) - \ddot{z}_{u,cg} \quad (4)$$

$$J_{pitch} \ddot{\theta} = T_{pitch} - J_{pitch} \ddot{\theta}_{u,cg} \quad (5)$$

$$J_{roll} \ddot{\phi} = T_{roll} - J_{roll} \ddot{\phi}_{u,cg} \quad (6)$$

How much the centers of mass of the unsprung and sprung bodies are off from one another in the vertical (Z), pitch (θ), and roll (ϕ) directions.

$$Z = z_{s,cg} - z_{u,cg} \quad (7)$$

$$\theta = \theta_{s,cg} - \theta_{u,cg} \quad (8)$$

$$\phi = \phi_{s,cg} - \phi_{u,cg} \quad (9)$$

Using the relative displacements, the following are the forces and moments acting on the sprung mass system:

$$F_{fl} = -k_f Z - b_f \dot{Z} + a k_f \theta + a b_f \dot{\theta} - l k_f \phi - l b_f \dot{\phi} \quad (10)$$

$$F_{fr} = -k_f Z - b_f \dot{Z} + a k_f \theta + a b_f \dot{\theta} + r k_f \phi + r b_f \dot{\phi} \quad (11)$$

$$F_{rl} = -k_r Z - b_r \dot{Z} - b k_r \theta - b b_r \dot{\theta} - l k_r \phi - l b_r \dot{\phi} \quad (12)$$

$$F_{rr} = -k_r Z - b_r \dot{Z} - b k_r \theta - b b_r \dot{\theta} + r k_r \phi + r b_r \dot{\phi} \quad (13)$$

$$T_{pitch} = -a(F_{fl} + F_{fr}) + b(F_{rl} + F_{rr}) \quad (14)$$

$$T_{roll} = -r(F_{fr} + F_{rr}) + l(F_{fl} + F_{rl}) \quad (15)$$

Research Methodology

Here, we'll go through the many sensors and other instruments that play a role in achieving this goal. The estimators' mathematical foundations are laid forth here as well.

Collection of Sensor Data

Synthetic sensor data is generated by a seven degrees of freedom car model driving down a simulated route. Using sine and cosine functions with frequencies of 0.77 Hz and 8.3 Hz and magnitudes of 3 cm and 0.3 cm, respectively, and step functions, a synthetic road profile is generated.

Methodology for Estimating Vague Variables

The dynamics of the model describe the parameters to be estimated as having unknown values. Generalized polynomial chaos is used as a mathematical approach to allow the uncertainty in the parameters to be transmitted to the model's dynamics (gPC). Setting initial values for the model's parameters, as illustrated in Equations (16)– (18), is the starting point.

$$Mass = \overline{mass} + \Delta_{mass} \quad (16)$$

$$J_{pitch} = \overline{J_{pitch}} + \Delta_{J_{pitch}} \quad (17)$$

$$J_{roll} = \overline{J_{roll}} + \Delta_{J_{roll}} \quad (18)$$

Due to the unpredictability of these factors, the answers to the differential equations will likewise be approximate. In gPC, the state space looks like this:

$$x = \left[\sum_{i=1}^S x_1^i \Psi^i(\xi) \dots \sum_{i=1}^S x_n^i \Psi^i(\xi) \sum_{i=1}^S v_1^i \Psi^i(\xi) \dots \sum_{i=1}^S v_n^i \Psi^i(\xi) \right]^T \quad (19)$$

Parameter values are explicitly added to the state space vector, which means:

$$x = \left[\sum_{i=1}^S x_1^i \Psi^i(\xi) \dots \sum_{i=1}^S x_n^i \Psi^i(\xi) \sum_{i=1}^S v_1^i \Psi^i(\xi) \dots \sum_{i=1}^S v_n^i \Psi^i(\xi) \right]^T \quad (20)$$

"state variable j" and "x I j," which stands for the i-th term of the power series. Similarly, v I j is the notation for the i-th term in the power series expansion of the j-th velocity variable in state space. P I d is the standard notation for parameter descriptions; d stands for the parameter index and I is the index of the power series coefficient. Each gPC series has an I() term that is the tensor product of the basis functions and the random variables that are used to span the range of the unknown parameters. Legendre polynomials and other orthonormal polynomials form the basis functions. See references [8, 18, 19, 23, 25] for further details. To get the coefficients of these power series, the collocation technique is used. Although there are several similarities between the collocation approach and Monte Carlo simulations, two important differences exist. We choose certain areas first. After that, all of the solutions are combined using the collocation matrix. It is possible to define the collocation matrix as follows:

$$A_{ji} = \Psi^i(\xi_j) \quad (21)$$

where the i-th index represents the basis functions' tensor project and the j-th index represents the points selected from the collocation points. The vectors representing the collocation points are as follows:

$$\xi^j = [\xi_1^j \dots \xi_d^j] \quad (22)$$

Where j is the row of points, in the range (1, j)S, and d is the index of the points picked for each unsure parameter. In most cases, 3S Q 4S collocations are necessary for a stable solution [5]. This leads to the following solution for the coefficients:

$$x^j(T) = \sum_{i=1}^Q (A^\#)_{ji} X^i(T) \quad (23)$$

The Moore-Penrose pseudo-inverse is denoted by A#. Using the i-th row vector of collocation points, we may derive the i-th set of state space parameters from the dynamics, denoted by x I and the j-the set of power series coefficients, denoted by x j.

methods of estimation

Section 4.2 demonstrates how the model's dynamics are affected by the uncertainty. Once the system is built, the result is a stochastic solution that does little more than spread the uncertainty about. The following two sections elaborate on the techniques used to make such estimates.

Adaptive Kalman Filtering with a Time Delay

To write out the state space form of a system of differential equations, one may say:

$$\dot{x} = f(x) + w \quad (24)$$

Where:

$$x = [x_1 \dots x_n, v_1 \dots v_n]^T \quad (25)$$

And w is the vector of process noise. The system measurement equation is defined as:

$$z = h(x) + v \quad (26)$$

The state vector is a part of an observed solution, represented by the observation matrix h. The sensor noise is denoted by the vector v. Linear systems are ideal for the Kalman Filter. The goal of the Extended Kalman Filter (EKF) is to create a roughly linear system by linearizing the system mechanics. This is achieved by doing a linearization of the system dynamics and evaluation of the observation matrices at each time step, k:

$$F_k = \left. \frac{\delta f(x)}{\delta x} \right|_{x=x_k} \quad (27)$$

$$H_k = \left. \frac{\delta h(x)}{\delta x} \right|_{x=x_k} \quad (28)$$

The EKF equation is:

$$\mathbf{x}_k^u = \mathbf{x}_k^f + K_k(z_k - H_k * \mathbf{x}_k) \quad (29)$$

The system takes the initial forecast (or model solution), \mathbf{x}_k^f , and updates it through the Kalman Update equations, K_k , and the residual, $(z_k - H_k * \mathbf{x}_k)$, to update the state variables, \mathbf{x}_k^u . The Kalman Update equation is defined as:

$$K_k = M_k H_k^T (H_k M_k H_k^T + R_k)^{-1} \quad (30)$$

The covariance matrices, M_k , and, P_k are thus obtained as:

$$M_k = \Phi_k P_{k-1} \Phi_k + Q_k \quad (31)$$

$$P_k = (I - K_k H_k) M_k \quad (32)$$

The system covariance matrix, M_k , is created through the functional matrix, Φ_k , and the forecasted system covariance, P_{k-1} . The R_k matrix is the measurement noise matrix, defined as:

$$R_k = E(\mathbf{v}\mathbf{v}^T) \quad (33)$$

E is the mathematical expectation operator. Q_k is the matrix that describes the discrete process noise matrix, through the process noise matrix, Q .

$$\Phi_k = e^{F_k T_s} \quad (34)$$

$$Q = E(\mathbf{w}\mathbf{w}^T) \quad (35)$$

$$Q_k = \int_0^{T_s} \Phi_k Q \Phi_k dt \quad (36)$$

More explicit detailing and implementation of the EKF can be found in [10, 22, 26].

The Generalized Polynomial Chaos – Extended Kalman Filter

The EKF equations are modified to accept the gPC power series solutions of the state variables. The gPC method calculates the covariances of the variables through multiplication of the power series coefficients as defined by Equation (37), for normalized basis functions:

$$cov(x_{d,k}, x_{j,k}) = \sum_{i=2}^Q x_{d,k}^i x_{j,k}^i \quad (37)$$

For gPC-EKF the Kalman Update equation is defined as:

$$\mathbf{x}_k^{u,i} = \mathbf{x}_k^{f,i} + K_k (z_k \delta(i-1) - H_k \mathbf{x}_k^{f,i}) \quad (38)$$

$$K_k = cov(\mathbf{x}_k^f, \mathbf{p}_k) H_k^T (R_k + H_k cov(\mathbf{x}_{1..2n}, \mathbf{x}_{1..2n}) H_k^T)^{-1} \quad (39)$$

More explicit derivation of this equation can be found in reference [3]. The indexes are defined as: The subscript k indexes time. The u and f superscripts denote the updated and forecasted state space vectors. The superscript i indexes the term of the power series. The $1 \dots 2n$ subscript denotes that only the state variables, and not the parameters are to be used here. T is the matrix transpose operator. The variables are defined as: z is the vector of the sensor signals. R is the sensor signal noise matrix δ is the dirac delta function H is the linearized observation matrix p is the vector of parameters.

Bayesian Statistics

Parameter values may be estimated using Bayesian Statistics. The method relies on the assumption that the discrepancy between the signal and the model follows a normal distribution. Parameter estimation within a Bayesian framework is described as:

$$P[p|z] = \frac{P[z|p]P[p]}{P[z]} \quad (40)$$

If you're only trying to get an idea of something's likely size, you may safely disregard the word $P[z]$ as a constant scaling factor. Because of this, we may simplify Equation (41) to:

$$P[p|z] \propto P[z|p]P[p] \quad (41)$$

The posterior density function of parameter values $P[p|z]$ is a statistical measure of how likely it is that a certain parameter value really exists, given the data. The statistical

distribution of the signal-to-model mismatch is denoted by the notation $P[z|p]$. This is defined given a normal distribution as:

$$P[z|p] = e^{-\frac{1}{2} \sum_{t=T_i}^{T_f} (z_t - h_t(x))^T R_t^{-1} (z_t - h_t(x))} \quad (42)$$

You may think of the signal at each time t as a vector z , and the model's output as a vector h . In this context, the signal-to-noise ratio is denoted by R_t . We talk about the prior distribution of parameters, $P[p]$. The states' vector is represented by the symbol x . This is a powerful tool inside the Bayesian paradigm as it considers previous knowledge about the parameter distributions. During this time, the estimator learns new things. Prior to calculating the probability distribution $P[p|z]$, a set of data covering the interval $[T_i \dots T_f]$ must be collected. The MAP estimation, which finds the parameters whose values maximize $P[p|z]$, is used. In order to arrive at the following estimate, we first get the distribution of $P[p]$ from its probability density function. The parameters, p , are not being estimated, but rather the values of the random variables. Because of this, Equation (29) takes on a new interpretation:

$$P[z|\xi] = e^{-\frac{1}{2} \sum_{t=T_i}^{T_f} (z_t - h_t(x, \xi))^T R_t^{-1} (z_t - h_t(x, \xi))} \quad (43)$$

$$P[\xi|z] \propto P[z|\xi] P[\xi] \quad (44)$$

The values of the state space variables (positions and velocities) and the parameters (mass, pitch inertia, and roll inertia) are returned by the collocation matrix using the MAP estimate of the random variables from Equation (31).

$$A(\xi_{Est}) x(t, \xi_{Est}) \quad (45)$$

Discussion of Simulated Outcomes

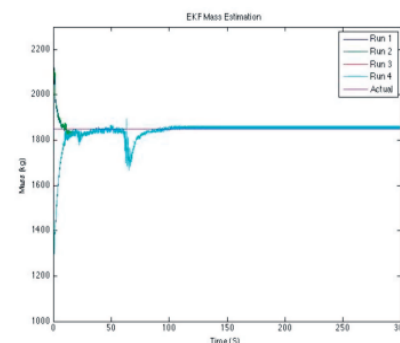
Obtaining Outcomes from an Extended Kalman Filter

The Extended Kalman Filter is used to run four distinct simulations. Parameter estimates for each simulation are shown in figures (3-5), and parameter ranges are included in Table 1. Initial approximations for the parameters are

established for the Mass, Pitch Inertia, and Roll Inertia. Mass, pitch inertia, and roll inertia have respective variances of 600 kilograms, 700 kilograms per square meter, and 400 kilograms per square meter.

Table 1. Variations in the parameters used as inputs for the EKF estimation simulations

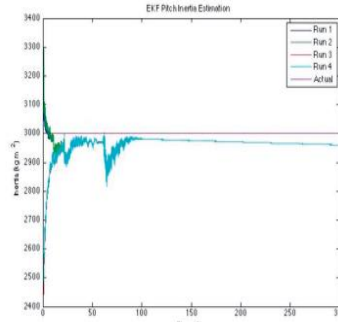
Run	Mass	Pitch Inertia	Roll Inertia	Poly Order
1	2250	3500	1100	2
2	2250	3500	1100	4
3	1500	2700	600	2
4	1500	2700	600	4



The estimated mass of the EKF as a function of time is shown in Fig. 3.

The time step of the integrator is precisely 0.005 seconds. The whole time is thirty-five seconds. The EKF estimations are very accurate if the models match well. Assumptions made during model building about sensor reading ranges cause EKF estimates to become less consistent. A speed bump causes a noticeable shift in parameter values at $t = 61s$, providing a clear example of this. To lessen the effect, one may either increase the polynomial order, modify the sensor noise matrix, or change the time step, or do all three. In the steady state, Table 2 shows the percentages by which the model parameters differ from the true value:

Fig. 4. pitch inertia



EKF

estimate versus time

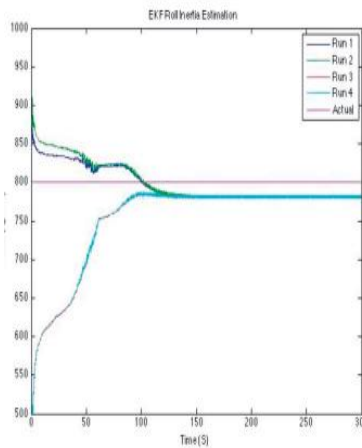


Fig. 5. EKF roll inertia versus time

Table 2. EKF error percentages for final estimation

Mass Error %	Pitch Inertia Error %	Roll Inertia Error %
0.01	-1.31	-2.27

Bayesian Statistics

Eight experiments are detailed below in Tables 3 and 4. For each of the estimation experiments, several of the parameters are changed. These are listed below as the initial estimation of the mass, pitch inertia and roll inertia mean values, the polynomial order (Poly Order) of the gPC expansions, the length of each time interProbability and Statistics with a Bayesian Twist

In Tables 3 and 4, we provide the results of eight separate trials. Several parameters are adjusted in each estimate experiment. Below

you'll find the initial estimates of mass, pitch inertia, and roll inertia, the polynomial order (Poly Order) of the gPC expansions, the duration of each time period utilized for estimation, and the total number of estimations.

val used for estimation and the number of estimations performed.

Table 3. Initial parameters fed into the Bayesian MAP estimation algorithm

Run	Mass	Pitch Inertia	Roll Inertia	Poly Order	Time Interval	# of Intervals
1	2250	3500	1000	6	24	1
2	2250	3500	1000	6	1	24
3	2250	3500	1000	4	24	1
4	2250	3500	1000	4	1	24
5	1650	2600	1000	6	24	1
6	2250	3500	1000	4	6	4
7	2250	3500	1000	4	60	1
8	2250	3500	1000	10	24	1

Table 3 details the results of the estimation algorithm. The table details what the final estimates are, and what their percent error is relative to the actual values of the synthetic data model. The estimate algorithm's output is listed in Table 3. In the table, you can see both the final estimates and the percentage error between the estimates and the real values of the simulated data set.

Table 4: The Bayesian Simulation Outcomes

Run	Mass Est	Pitch Est	Roll Est	% Err Mass	% Err Pitch	% Err Roll
1	1905.685	3054.9	785.44	3.01%	1.83%	-1.82%
2	1897.915	3017.19	823.28	2.59%	0.57%	2.91%
3	1934.36	3159	780.08	4.56%	5.3%	-2.49%
4	1852.405	2877	833.44	0.13%	-4.1%	4.18%
5	1914	3069.4	766.7	3.46%	2.31%	-4.17%
6	1897.9	3048.3	858.2	2.59%	2.61%	7.28%
7	1802.5	2876.4	803.4	-1.59%	-4.12%	0.43%
8	1874.2	3047.3	777.7	1.31%	1.58%	-2.78%

Evidence suggests that estimates improve with increasing polynomial order. The mathematics suggests that this conforms to the expected behavior of the gPC. In line with statistical theory, the accuracy of the estimate produced by the Bayesian estimating method improves

with the length of the time sequence supplied into it. It is also clear that the guess is more precise the more precise the first estimate is.

Conclusions

In this research, we construct a model of a vehicle that can predict its mass, pitch inertia, and roll inertia using a sparse set of sensors and an absence of a terrain profile. The procedures carried out provide satisfactory outcomes, and the final model exhibits good correlation with the seven degrees of freedom model. The Bayesian model outperforms the EKF model in terms of reliability. You can make EKF models run faster and show you the effects of changing parameters in real time.

REFERENCES

[1] *Using Polynomial Chaos Theory for Recursive Bayesian Parameter Estimation*, B.L. Pence et al., 2010.

[2] *in Parameter Estimation Methods Based on Polynomial Chaos and Their Applications to Vehicle Systems* by Blanchard, Sandu, and Sandu, C. the 2009 edition of IMechE, Vol. 223.

the third *Using a Polynomial Chaos-Based Kalman Filter Approach*, Blanchard, Sandu, and Sandu C. developed PSM, a method for estimating mechanical system parameters. Volume 132, 2010 of the *Journal of Dynamic Systems, Modeling, and Control*.

[4] Cheng H., Sandu A.: *How to efficiently quantify uncertainty in stiff systems using the polynomial chaos approach*. Volume 79, Issue 3, 2009, Pages 3278–3295 of *Mathematics and Computers in Simulation*.

Cheng and Sandu's work on quantifying uncertainty in three-dimensional air quality models using polynomial chaos is cited as [5]. *Modeling and Software for the Environment*, 2009.

[6] *Influence of Parameter Variation for System Identification of Pitch-heave Car Model*, 2010 (Cui Y., Kurfess T.R.).

[7] *Estimating the Mass of Vehicles Online using Recursive Least Squares and Supervisory Data Extraction* (Farthy, Kang, & Stein, 2016). *Conference on American Control*, 2008.

Parametric Optimal Design of Uncertain Dynamical Systems, 2011 (Hays J., 2013).

The third section, S.K.S., deals with the adaptive polynomial-chaos method for estimating the vehicle's spring mass parameters.

[10] *A Novel Application of the Kalman Filter to Nonlinear Systems* by Julier S.J. and Uhlmann J.K.

[11] *In their work on optimizing parameter estimates for DC motors*, Lankarany and Rezazade use a genetic method. 2007 *IEE International Conference on Electrical and Electronics*(2007).

[12] *Stochastic spectrum approaches for efficient Bayesian solution of inverse problems* (Y.M. Marzouk, H.N. Najm, and L.A. Rahn, 2017). Published in 2007 in the *Journal of Computational Physics*, Volume 224, Pages 560–586.

One method for estimating vehicle mass and road grade is a two-stage Lyapunov-based estimator [13] developed by McIntyre, Ghotikar, Vahidi, Song, and Dawson, Darren. published in the *IEEE Transactions on Vehicle Technology*, volume 58, page 200.

Sigma-Point Kalman Filters for Nonlinear Estimation and Sensor-Fusion - Applications to Integrated Navigation [14] Merwe R.v.d., Wan E.A., Julier S.I.

The authors of the 2011 paper "Vehicle Sprung Mass Estimation for Rough Terrain" are Pence, Hays, Fathy, Sandu, and Stein.

An Approach to Base-Excitation for Polynomial Chaos-Based Sprung Mass Estimation in Off-Road Vehicles [16] (Pence, Fathy, & Stein, 2017).

[17] Rozyn and Zhang: *An approach to estimating the inertial characteristics of vehicles*. Chapter 48, Pages 547–565, in *Vehicle System Dynamics*, 2010.

A. Sandu, C. Sandu, and M. Ahmadian: *Uncertainty-Based Modeling of Multibody Systems* [18]. Section One: *A Look at the Mathematical and Experimental Details*. *Dyn Multibody*, 2006.

The year 19 Part II: Numerical applications of Sandu, A., and Ahmadian's model for the modeling of multibody systems with uncertainties. Article published in 2006 in the journal Multibody System Dyn.

In [20], Using polynomial chaos expansions for real-time parameter identification, Southward S.C. 2007 American Society of Mechanical Engineers Annual Conference and Exposition.